Journal of Intelligent Materials Systems and Structures
Vol. xx, No. xx, pp. xxx-xxx, 2014

Application of Preview Information to Pointing Control of Truss Structure Using Artificial Thermal Expansion on Orbit

By Yusuke FUNAKOSHI[1)], Kosei ISHIMURA[2)], Yoshiro OGI[3)], Takashi IWASA[4)]

[1)]*Department of Aeronautics and Astronautics, The University of Tokyo, Tokyo, Japan*
[2]*Institute of Space and Astronautical Science, Japan Aerospace Exploration Agency, Kanagawa, Japan*
[3)] *Institute of Industrial Science, The University of Tokyo, Tokyo, Japan*
[4)]*Department of Mechanical Engineering, Tottori University, Tottori, Japan*

Abstract

The pointing performance of a truss structure on orbit that is used for a large space telescope is discussed. To achieve advanced science missions, large and precise support structures such as truss structures are needed. However, the preciseness of the structure might be lost due to various disturbances on orbit. Therefore, to realize ultra-large and precise support structures, active shape control of the structures is needed. To control the shape, we use artificial thermal expansion caused by heaters instead of mechanical actuators. Control systems without mechanical mechanisms have high reliability, which is very attractive for use on orbit. However, there are some constraints regarding the usage of heaters. The control input is restricted to positive inputs because heaters can give off heat but cannot dissipate heat actively, and there will be upper limits on the heat input. To improve the control performance under such constraints, we apply "Model Predictive Control (MPC)" as a feedforward control method with preview information. In this paper, we mainly show the effectiveness of MPC compared with PI control, which is one of the typical feedback control methods. We developed a structural mathematical model and a thermal mathematical model in order to evaluate the performance of the control system. It is confirmed through numerical simulations that the total error is reduced by MPC compared with PI control.

Key Words: Pointing control, Large space telescope, Thermal expansion, Preview information, Model predictive control

1. Introduction

In order to achieve advanced space science missions, large structures that have both high reliability and high shape stability are needed (Agnes and Dooley, 2004; Puig et al., 2010). However, the preciseness of the structural shape might be lost due to various disturbances on orbit. Such fluctuations in structural shape are classified by time scale: short-term fluctuations caused mainly by micro vibration, middle-term fluctuations caused mainly by thermal deformation, and long-term fluctuations caused mainly by the aging and degradation of the materials. Traditionally, passive control methods for each factor have been adopted to achieve the structural requirements. However, it is becoming increasingly difficult to achieve the requirements with only passive control methods because the requirements have rapidly advanced in recent years. Therefore, to realize ultra-large and precise structures in the future, active shape control of the structures (that is, a smart structural system) is needed (Miura, 1992; Wada et al, 1990; Utku and Wada, 1993; Lake et al., 1998; Korkmaz, 2011).

Maintaining pointing performance is one of the major requirements for space science missions using large and precise space telescopes. However, it is very difficult to maintain the precise pointing performance of large structures such as the next international X-ray astronomy satellite (ASTRO-H) being developed by JAXA (Takahashi et al., 2010). In this research, therefore, we control the shape of the truss structure, which is generally used as a support structure on orbit, focusing on the pointing performance. The purpose of this research is to maintain pointing performance, especially against middle-term fluctuation caused by thermal deformation (Tolson and Huang, 1992; Givoli and Rand, 1995). Only quasi-static motion is considered because we assume that the objective structure has a sufficiently high natural frequency compared with the thermal time constant. We use heaters as the control actuators for the smart structural system and conduct pointing control by artificial thermal expansion (Haftka and Adelman, 1985; Edberg, 1987; Pichler and Irschik, 2001). Such an actuator system is expected to have high repeatability and high reliability because there are no movable mechanisms. These characteristics are very attractive for spacecraft structures. On the other hand, the control system that we propose has a problem in its response time because the control input is restricted to positive inputs. Although temperature rises can be controlled by the heater, it is difficult to control temperature drops. Therefore, for practical use, a novel control system that can overcome this problem is required. At first, we had performed some pointing control experiments for a 1.9 m high truss structure with a simple PI controller. The performance using artificial thermal expansion for pointing control was investigated (Ishimura

et al., 2010, 2011). As a result, it was shown pointing control is possible within a 1% error against a 0.1 mm-order displacement using artificial thermal expansion. The achieved accuracy may be sufficient based on recent requirements for 10 m class space telescopes. However, significant overshoot can occur in attempts to achieve a quick response because we cannot actively add negative heat input. To reduce the overshoot, it is important for the control system to predict the future state and determine the control input based on the prediction.

The purpose in this paper is to improve the control performance by applying a predictive control system. Because thermal disturbances on orbit change periodically, the incorporation of preview information of thermal disturbances into the predictive control is expected to be effective. We adopt "Model Predictive Control (MPC)" as feedforward control that can incorporate preview information. Through numerical simulations, we will ascertain the effectiveness of the proposed control system. The MPC controller predicts the future state and determines the control input by comparing the predicted future state and the target state. Moreover, MPC has two advantages. One is the simplicity of incorporating constraints given by linear inequalities into the controller, and the other is the ability to control optimally under predictable disturbances. In other words, MPC can conduct optimum control considering the constraints of the actuator system and preview information of thermal disturbances. In this paper, we show the effectiveness of MPC through numerical simulations that apply it to a smart structural system.

2. Simulation Model and Governing Equations

2.1. System Diagram

Figure 1 shows a block diagram of the control system. In Fig. 1, the actuator corresponds to the heaters, and the plant corresponds to the structural system. The controller determines the control input, which is the applied voltage of the heaters, comparing the reference and measured outputs. The added heat from the heaters causes thermal deformation of the structural system. In the measurement system, the sensors measure the thermal deformation of the structural system.

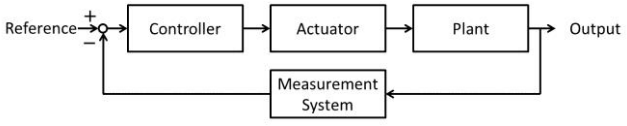

Fig. 1. System block diagram

We construct a thermal mathematical model and a structural mathematical model to simulate the thermal deformation. The thermal mathematical model is constructed based on the thermal equation, and the structural mathematical model is constructed based on the finite element method (FEM). In the simulation, we do not consider any noise in the measurement system. We use MATLAB/Simulink as the simulation tool in this research.

2.2. Thermal Equation

First, we formulate the thermal equation of the structural system on orbit. For the external heat input, solar radiation, earth radiation, albedo, and heat transfer from other satellite equipment are considered. The total external heat input is expressed as the thermal disturbance q_d. Furthermore, for the cooling effect, we consider only the heat radiation to space. Therefore, with a control heat input q_u, the thermal equation for the structural system on orbit is derived as follows:

$$C\frac{dT}{dt} = q_u(t) + q_d(t) - \sigma\varepsilon A_s(T^4 - T_a^4) \tag{1}$$

where A_s is the surface area, C is the heat capacity, T_a is the ambient temperature, ε is the emissivity, and σ is the Stefan-Boltzmann constant. For the comprehensive discussion, each of the physical variables is transformed to a non-dimensional variable. The non-dimensional physical variables $\hat{T}, \hat{t}, \hat{q}_u, \hat{q}_d$ are defined as

$$\hat{T} \equiv \frac{T}{T_0}, \quad \hat{t} \equiv \frac{t}{t_0}, \quad \hat{q}_u \equiv \frac{q_u}{q_0}, \quad \hat{q}_d \equiv \frac{q_d}{q_0}. \tag{2}$$

Here, T_0, t_0, and q_0 indicate the reference values for the temperature T, time t, and heat quantities q_u, q_d, respectively. With these non-dimensional variables, we can transform Eqn. (1) to obtain the following equation:

$$\frac{d\hat{T}}{d\hat{t}} = \hat{q}_u(\hat{t}) + \hat{q}_d(\hat{t}) - \frac{1}{r_1}(\hat{T}^4 - r_2^4) \tag{3}$$

where r_1, r_2 are non-dimensional quantities defined as

$$r_1 \equiv \frac{\tau_2}{\tau_1}, \quad r_2 \equiv \frac{T_a}{T_0} \tag{4}$$

and where τ_1, τ_2 have the dimension of time and are defined as

$$\tau_1 \equiv \left(\frac{q_0}{CT_0}\right)^{-1}, \quad \tau_2 \equiv \left(\frac{\sigma\varepsilon A_s T_0^3}{C}\right)^{-1}. \tag{5}$$

The physical meaning of τ_1 is the time required to raise the temperature by T_0 with a constant heat input of q_0. The physical meaning of τ_2 is the time constant of the temperature drop if only heat radiation is considered for heat transfer. To obtain Eqn. (3), it is assumed that $t_0 = \tau_1$ because we can select the reference values freely.

In the above transformations, there is no approximation because we only conduct changes in variables. However, in order to apply Eqn. (3) to the control system, some approximations (that is, linearization and discretization) are required. Considering the first term of the Taylor expansion and using forward difference approximation, we obtain the objective equation as follows:

$$\Delta\hat{T}(k+1) = (1-\frac{\Delta\hat{t}}{r_1})\Delta\hat{T}(k) + \Delta\hat{t}\,\hat{q}_u(k) + \Delta\hat{t}\left(\hat{q}_d(k) - \frac{1-r_2^{\,4}}{4r_1}\right) \quad (6)$$

where k indicates the time step, and $\Delta\hat{T}$ is a non-dimensional perturbation of the temperature around T_0 defined as $\Delta\hat{T} \equiv (T-T_0)/T_0$.

2.3. Model Predictive Control (MPC)

The MPC controller evaluates the difference between the predicted future state and the target state. Figure 2 shows the concept of MPC. The MPC controller calculates the difference between the predicted value and the reference value in the H_p finite steps for prediction, where H_p is the parameter called the predictive horizon, which determines the number of predictive steps. The reference trajectory is derived from the set-point trajectory. Then, the MPC controller determines the control input from k to $k+H_u$ to minimize the difference, where H_u is the parameter called the control horizon, which determines the number of control steps. However, the calculated control inputs are applied not in all of the steps but in the most recent step. The other following control inputs are used only for evaluation. In the next calculation time step, the controller performs the calculation again in the same way using the updated information. The advantages of MPC is the ease of incorporating constraints given by a linear inequality into the controller and being able to control optimally based on predictable disturbances.

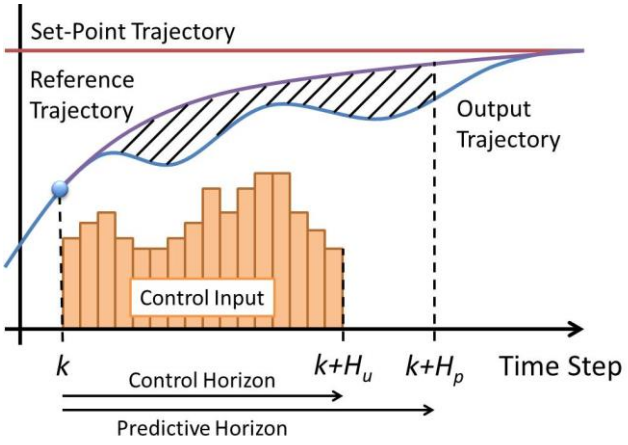

Fig.2. Model Predictive Control (MPC)

Here, we show an overview of the formulization for MPC. Please refer to the reference (Maciejowski, 2002) for more details. Consider that the state space equations are as follows:

$$\begin{cases} \tilde{\boldsymbol{x}}(k+1\,|\,k) = \boldsymbol{A}\,\tilde{\boldsymbol{x}}(k\,|\,k) + \boldsymbol{B}\,\boldsymbol{u}(k) + \boldsymbol{B}_d\boldsymbol{d}_m(k) \\ \tilde{\boldsymbol{z}}(k+1\,|\,k) = \boldsymbol{C}_z\,\tilde{\boldsymbol{x}}(k\,|\,k) \end{cases} \quad (7)$$

where $\tilde{\boldsymbol{x}}(k+i|k)$ and $\tilde{\boldsymbol{z}}(k+i|k)$ represent the state and output variables, respectively, at time $k+i$ ($i \geq 1$), which is predicted at time k, $\boldsymbol{u}(k)$ is the control input at time k, and $\boldsymbol{d}_m(k)$ is the disturbance at time k. In the case of the thermal deformation problem, the state variables are perturbations of temperature, and the output variables are displacements. Equation (6) can be used to predict the perturbation of temperature. The state variables, input variables, and disturbances correspond to the following variables:

$$\tilde{\boldsymbol{x}} = \Delta T,\ \boldsymbol{u} = q_u,\ \boldsymbol{d}_m = \left(\hat{q}_d - \frac{1-r_2^{\,4}}{4r_1}\right).$$

Moreover, the coefficients correspond to the following constants in our problem:

$$\boldsymbol{A} = (1-\frac{\Delta\hat{t}}{r_1}),\ \boldsymbol{B} = \Delta\hat{t},\ \boldsymbol{B}_d = \Delta\hat{t}\,.$$

In addition, as described in Section 2.2, we can obtain a non-dimensional equation of the structural mathematical model using FEM by similar procedures. In this research, $\boldsymbol{z}$ in Eqn. (7) corresponds to the pointing error caused by the thermal deformation of the structure. Therefore, $\boldsymbol{C}_z$ in Eqn. (7) is the transformation matrix from the temperature to the pointing error of the structure. These non-dimensional thermal and FEM equations correspond to the state space equations. Introducing the proper weighting functions, the evaluation function of control is defined as:

$$V(k) \equiv \sum_{i=0}^{H_p}\left[\tilde{\boldsymbol{z}}(k+i\,|\,k) - \boldsymbol{r}(k+i\,|\,k)\right]^T Q(i)\left[\tilde{\boldsymbol{z}}(k+i\,|\,k) - \boldsymbol{r}(k+i\,|\,k)\right] + \sum_{i=0}^{H_u-1}\Delta\tilde{\boldsymbol{u}}(k+i\,|\,k)^T R(i)\Delta\tilde{\boldsymbol{u}}(k+i\,|\,k) \quad (8)$$

where $Q(i)$ and $R(i)$ are weight functions at time $k+i$, and these functions have a general matrix form. These weight functions are determined considering the importance of the state variables at that time. Introducing the proper matrices $\boldsymbol{H}$, $\boldsymbol{G}$, Eqn. (8) is transformed into quadratic form as follows:

$$V(\Delta\boldsymbol{U}(k)) = \Delta\boldsymbol{U}(k)^T\boldsymbol{H}\Delta\boldsymbol{U}(k) - \Delta\boldsymbol{U}(k)^T\boldsymbol{G} + Const \quad (9)$$

where $\Delta\boldsymbol{U}(k) \equiv [\Delta\tilde{\boldsymbol{u}}(k\,|\,k) \ \cdots \ \Delta\tilde{\boldsymbol{u}}(k+H_u-1\,|\,k)]^T$. The $\Delta\boldsymbol{U}(k)$ that minimizes the evaluation function Eqn. (9) is the optimum control input. Practically, the control input often has some constraints. In this research, the constraints given by the linear inequality are considered. In the case of a heat input, there are upper and lower limits as follows:

$$0 \leq u(k+i\,|\,k) \leq u_{\max} \ \text{ for } \forall i\,. \quad (10)$$

Equation (10) is transformed into the following matrix form:

$$\begin{bmatrix} -1 & 0 \\ 1/u_{\max} & -1 \end{bmatrix} \begin{bmatrix} u(k+i\,|\,k) \\ 1 \end{bmatrix} \le \mathbf{0}\,. \tag{11}$$

Considering Eqn. (11) in each step until H_u and then using proper matrices, we can obtain the following equation:

$$[\boldsymbol{F}_1 \quad \boldsymbol{F}_2 \quad \cdots \quad \boldsymbol{F}_{H_u} \quad \boldsymbol{f}] \begin{bmatrix} \boldsymbol{u}(k) \\ 1 \end{bmatrix} \le \mathbf{0} \tag{12}$$

where $\boldsymbol{u}(k) \equiv [\tilde{\boldsymbol{u}}(k\,|\,k) \quad \cdots \quad \tilde{\boldsymbol{u}}(k+H_u-1\,|\,k)]^T$, $\boldsymbol{F}_i$ is the column vector corresponding to the values of the constraints in the i[th] step, and $\boldsymbol{f}$ is also a column vector, where the signs of its elements depend on the direction of the original inequalities as constraints. Furthermore, by transforming Eqn. (12), we obtain the following equation:

$$\boldsymbol{F}\,\Delta\boldsymbol{u}(k) \le \boldsymbol{F}_1\,\boldsymbol{u}(k-1) - \boldsymbol{f} \tag{13}$$

where $\boldsymbol{F}, \boldsymbol{F}_1$ are defined as:

$$\begin{aligned} \boldsymbol{F}_i &\equiv \sum_{j=i}^{H_u} \boldsymbol{F}_j \\ \boldsymbol{F} &\equiv \begin{bmatrix} \boldsymbol{F}_1 & \boldsymbol{F}_2 & \cdots & \boldsymbol{F}_{H_u} \end{bmatrix}. \end{aligned} \tag{14}$$

Finally, the following equations are obtained:

Minimize

$$V(\Delta\boldsymbol{u}(k)) = \Delta\boldsymbol{u}(k)^T\,\boldsymbol{H}\,\Delta\boldsymbol{u}(k) - \Delta\boldsymbol{u}(k)^T\,\boldsymbol{G} \tag{15}$$

subject to

$$\boldsymbol{F}\,\Delta\boldsymbol{u}(k) \le \boldsymbol{F}_1\,\boldsymbol{u}(k-1) - \boldsymbol{f}\,.$$

The optimum control input is determined uniquely by solving the quadratic programming problem defined in Eqn. (15). The parameters of the control system that we can design are the predictive horizon H_p, control horizon H_u, and weight functions $Q(i)$ and $R(i)$ against the evaluation function.

3. Fundamental Characteristics of MPC

3.1. Control of Rod Length

In order to investigate the fundamental characteristics of the MPC, we conduct a control simulation of a simple structure. We apply MPC to the shape control of the length of a rod. Figure 3 shows the model of the rod, and Table 1 shows the conditions of the simulation. These parameters are determined to make the system stabilize considering the general standard of the control parameters (Franklin et al., 2009; Maciejowski, 2002). In fact, these parameters have not been fully optimized but have been nearly optimized. In this simulation, it is assumed that the rod deforms only along the longitudinal direction. We control the displacement of the tip of the rod to keep it constant by controlling the heat input. The thermal disturbance is added as a periodical step function. We have four kinds of measurable variables in the MPC; the first one is the temperature of the structural member, the second one is the displacement of the target point, the third one is the control input in the previous time steps, and the last one is the pointing error of the structure. In addition to these, the disturbance (in this case the heat input) can be predicted, although it cannot be measured. The period is expressed as τ_d, which is obtained by dividing the original period by τ_1. In order to compare the control performance, we prepare two controllers, which are PI and MPC controllers. We assume that the root of the rod is insulated, and there is no temperature distribution in the longitudinal direction. Only radiation is taken into account.

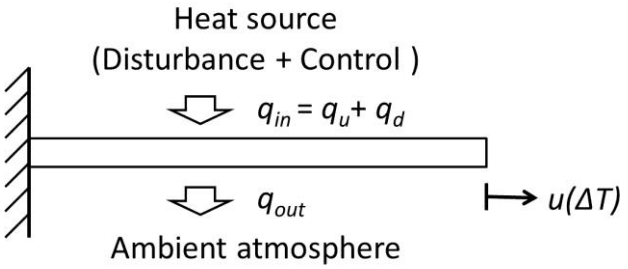

Fig. 3 Control of rod length

Table 1 Conditions of model and controllers

Model Parameters	PI Parameters	MPC Parameters
$r_1 = 0.1$	$K_P = 10^3$	$H_p = 100$
$r_2 = 1$	$K_I = 1.5\times10^4$	$H_u = 10$
$\hat{\tau}_d = 1$		$Q(i) = 10^3 \times 1.5^{(1-i)}$
$\hat{q}_{u\max} = 10$		$R(i) = 0$

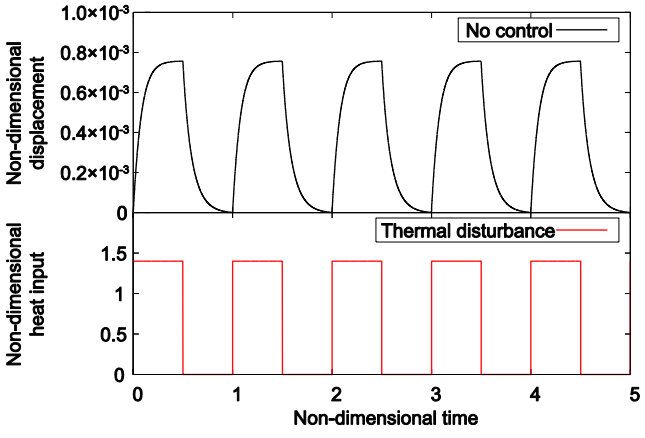

Fig. 4. Thermal disturbance and induced non-dimensional displacement

Figure 4 shows the added thermal disturbance for the rod and the induced displacement. In the case of no control, the induced displacement increases at the same time as the heating starts and then decreases exponentially

after the heating stops. We designed both PI and MPC controllers to maintain the non-dimensional displacement at 1.0×10^{-3}. Both cases are simulated numerically.

Figure 5 shows the displacements of each case for the PI and MPC controllers, respectively. In the case of PI control, it is found that large leaps are generated immediately after thermal disturbance changes. Moreover, the tails of the leaps remain for a long period of time. On the other hand, in the case of MPC, the generated leaps are small and vanish over very short amounts of time. This is because MPC can begin control in advance by predicting the change in thermal disturbance and the future state. The displacement controlled by MPC converges to a bias point slightly apart from the set-point. The bias error is only on the order of 0.1%. This is caused by the modeling error due to approximation, that is, the linearization of the nonlinear equation. As a result, it is concluded that MPC could control this system with high accuracy.

Figure 6 shows the heat inputs of the control. In Fig. 6, the heat inputs given by the PI and MPC controllers seem to be almost the same in this time scale. On the contrary, the behaviors of the heat inputs given by the PI and MPC controller are dramatically different around the instants when the thermal disturbance changes. Figure 7 shows enlarged views of Fig. 6 around the instant when the thermal disturbance changes. As shown in Fig. 7, the MPC controller begins control previous to the change in thermal disturbance. Because of such feedforward inputs, MPC can control more quickly than PI control.

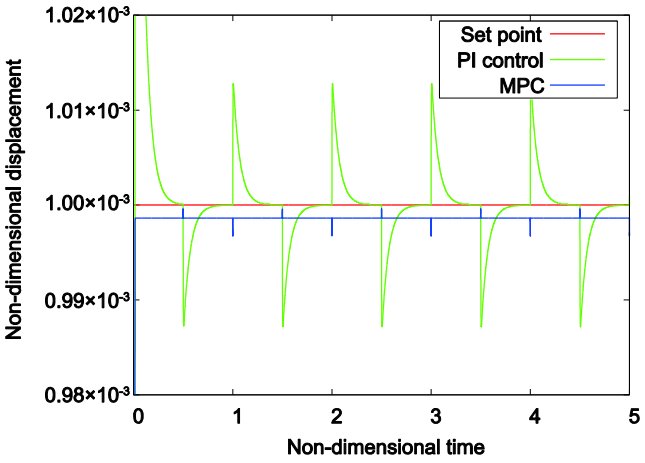

Fig. 5 Non-dimensional displacements controlled by PI and MPC controllers

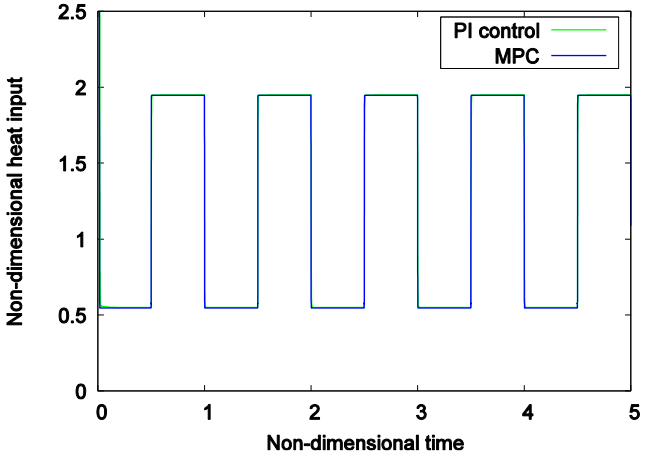

Fig. 6. Control heat inputs

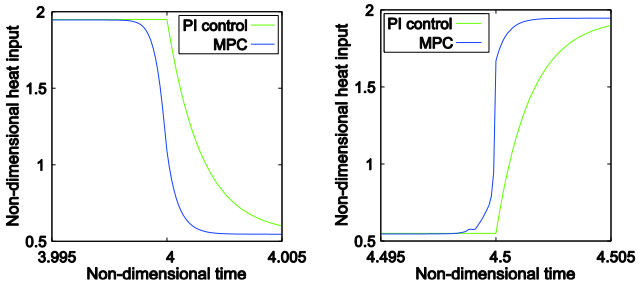

(a) Around rise of thermal disturbances

(b) Around fall of thermal disturbances

Fig. 7. Enlarged views of control heat inputs

We evaluate the control performance using the following parameters:

$$e \equiv \frac{1}{\hat{\tau}_d}\int_{\hat{\tau}_d} (\hat{\delta}_{set} - \hat{\delta})^2 d\hat{t} \tag{16}$$

$$\hat{q}_{u,total} \equiv \int_{\hat{\tau}_d} \hat{q}_u(\hat{t}) d\hat{t} \tag{17}$$

where $\hat{\delta}_{set}$ is the non-dimensional displacement of the set-point, and $\hat{\delta}$ is the non-dimensional displacement of the output, which means thermal strain is defined as the displacement divided by the original length of the rod. Here, e indicates the variance of errors in displacement over one cycle, and $\hat{q}_{u,total}$ indicates the total amount of heating for control over one cycle. We summarized e and $\hat{q}_{u,total}$ after the transient response in Table 2.

Table 2 Performance of PI control and MPC

	PI control	MPC
e	$1.3.\times10^{-7}$	0.2×10^{-7}
$\hat{q}_{u,total}$	1.25	1.25

The total amount of heating is no different between the case using PI control and that using MPC. However, there is a significant difference in the errors. The MPC controller reduced the error to less than 1/6 of that of the PI controller with no difference in the amount of heating.

3.2. Sensitivity of Control Performance to Parameters

It is expected that the above results might change depending on the parameters of the state-space equations and controllers. We analyze the sensitivity of the control performance to each parameter. Structures on orbit are almost in periodic steady state. Therefore, not a transient state but a periodic steady state is used for the performance evaluation. We analyzed the sensitivity of the control performance by independently varying each parameter of the model. The parameters that we varied are r_1, r_2, $\hat{q}_{u\,max}$, and $\hat{\tau}_d$. The physical meaning of each parameter is as follows: r_1 is the ratio of required time for heating to the radiation, r_2 indicates the net heat transfer between the structure and the ambient temperature, $\hat{q}_{u\,max}$ indicates the maximum control heat input (that is, a model that has a larger $\hat{q}_{u\,max}$ has plenty more resources for control), and $\hat{\tau}_d$ indicates the ratio of the time scale of the disturbance with respect to $\hat{\tau}_1$.

Figure 8 shows the results of the sensitivity analysis for each parameter. In Fig. 8, each parameter is set as the horizontal axis, and e_{MPC}/e_{PI}, which is the ratio of errors for the PI control and MPC, is set as the vertical axis. $e_{MPC}/e_{PI} = 1$ indicates that the errors of the PI control and MPC have no difference, and a lower value of e_{MPC}/e_{PI} indicates that the MPC works more effectively than the PI control. As a result, it is found that MPC has very high control performance for all of the parameters except one case.

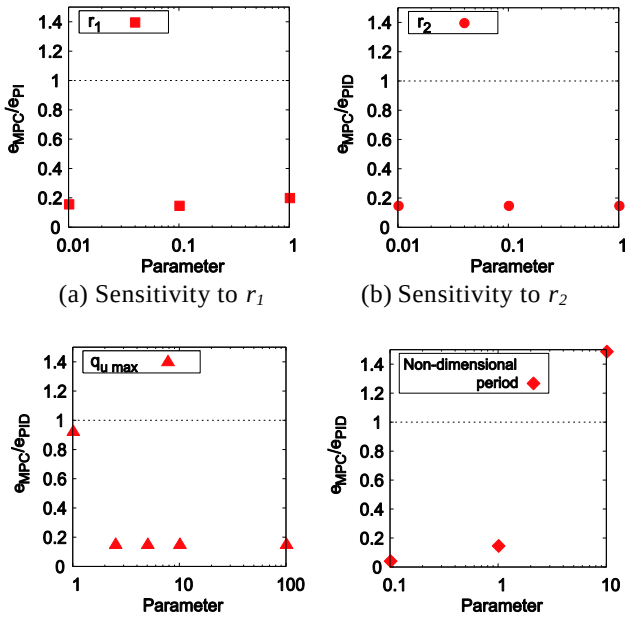

(a) Sensitivity to r_1 (b) Sensitivity to r_2

(c) Sensitivity to $\hat{q}_{u,\max}$ (d) Sensitivity to $\hat{\tau}_d$

Fig. 8. Sensitivity to each parameter

The exception is observed in the case of the sensitivity to $\hat{\tau}_d$. Figures 9 and 10 show the behaviors of the control in the case of $\hat{\tau}_d = 0.1$ and $\hat{\tau}_d = 10$, respectively. If the period of the thermal disturbance is shorter than the required time for convergence against the overshoot, the PI controller cannot follow such a thermal disturbance sufficiently. However, if the period of the thermal disturbance becomes slower, the PI controller works sufficiently. On the other hand, MPC shows the opposite characteristics. Independently of the period of the thermal disturbance, the MPC controller can follow the change in thermal disturbance, as shown in Figs. 9 and 10. However, the bias error remains in both cases. Therefore, in the case of $\hat{\tau}_d = 10$, e_{MPC} seems to be larger than e_{PI}. Such bias errors can be excluded by considering an artificial offset in the reference trajectory as referred to in the reference (Maciejowski, 2002).

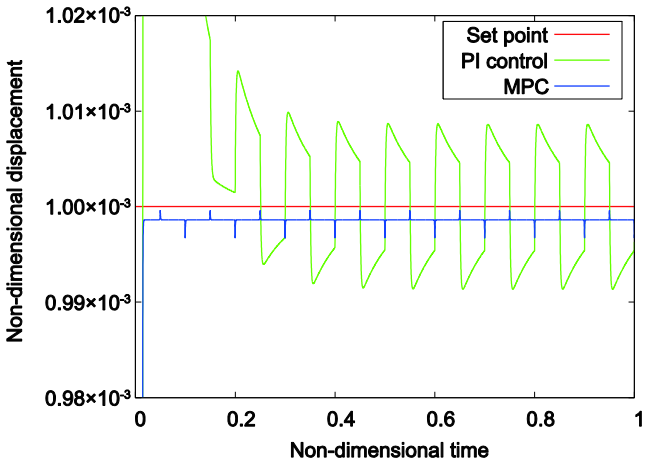

Fig. 9. Non-dimensional displacements in the case of $\hat{\tau}_d = 0.1$

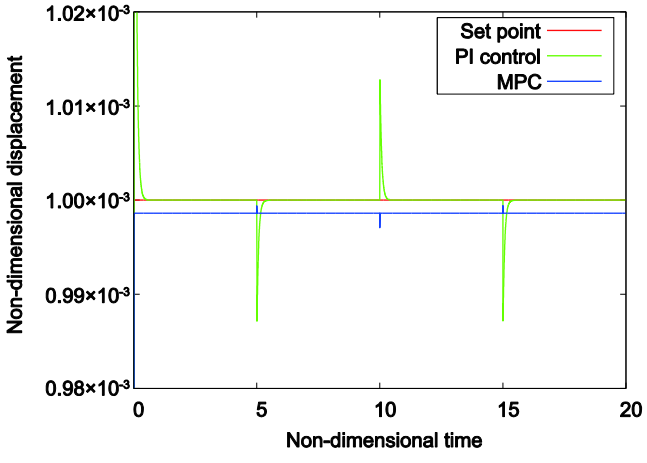

Fig. 10. Non-dimensional displacements in the case of $\hat{\tau}_d = 10$

4. Pointing control of truss structure

In order to demonstrate the performance of MPC in practical use, we apply MPC to the pointing control of the truss structure shown in Fig. 11. It is assumed that the displacement of the target point against the base point shown in Fig. 11 corresponds to the fluctuation of the pointing axis. We also use both the PI and MPC controllers for comparison. The truss structure is a statically indeterminate structure constructed of 65 members and has symmetry in the x and y directions.

The physical properties of this structure and model are shown in Table 3. It is assumed that the truss structure has ideal pointing performance in its initial state. Therefore, the displacements of the target point in the x-y plane are zero at the set-point state in this control. In this simulation, four members at the bottom are selected for heating. It is assumed that the heat inputs from heaters 3 and 4 correspond to thermal disturbances. Thermal disturbances are given as a step function or a sinusoidal function. The step function simulates rapid thermal changes caused by an eclipse, and the sinusoidal function simulates gradual changes due to albedo and so on. We control the displacements by using heaters 1 and 2 as actuators. Because the truss structure has symmetry, each heater can control the displacement only in the diagonal direction.

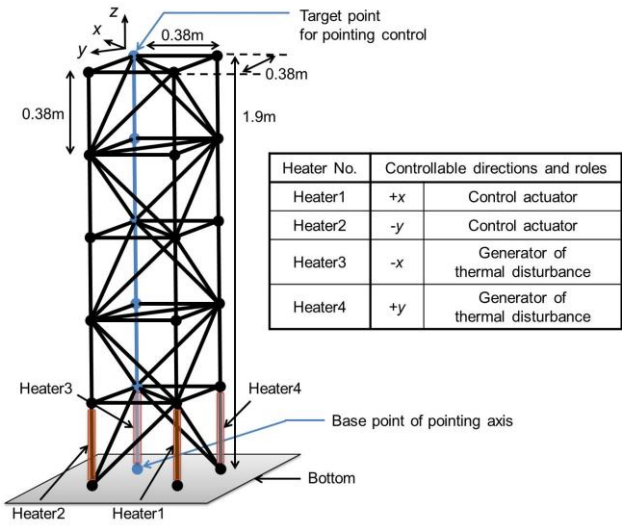

Fig. 11. Truss structure model for simulation

Table 3 Properties and conditions of truss structure model

Properties of truss members	
Length of axial members	0.38 m
Length of diagonal members	0.54 m
Heat capacity of axial members	30 J/K
Surface area of axial members	0.01 m^2
Tensile stiffness	1.99×10^{6} N
Coefficient of thermal expansion	2.15×10^{-5} K^{-1}
Absorptivity	0.12
Emissivity	0.3
Condition	
Ambient temperature	273 K

Case 1: Thermal disturbance given as step function

In case 1, we discuss the control behaviors when thermal disturbances are given as step functions, as shown in Fig. 12. Figure 13 shows the induced displacements without a controller. It is found that the displacements in both the x and y directions change depending on the thermal disturbance. At first, the average temperature increases transiently; then, it settles in a periodic steady state. Therefore, after sufficient time, the displacements begin to change periodically.

Figure 14 shows the displacements controlled by the PI controller. Large leaps are periodically generated because the control heat inputs are added only after the displacements have changed. Moreover, it takes a long time for convergence. Figure 15 shows the displacements controlled by the MPC controller. The displacements properly converge at the set-point with MPC. In the case of MPC, we can observe the large leaps just before the thermal disturbance changes, but these behaviors are essentially different from that of PI control. The purpose of these behaviors is to prepare the coming change in thermal disturbance. Therefore, the controlled displacements with MPC can quickly converge to the set-point, although large leaps occur instantly.

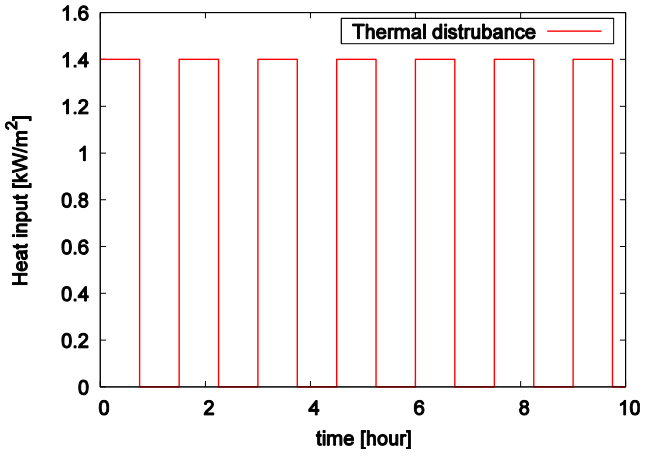

Fig. 12. Thermal disturbance given as step function

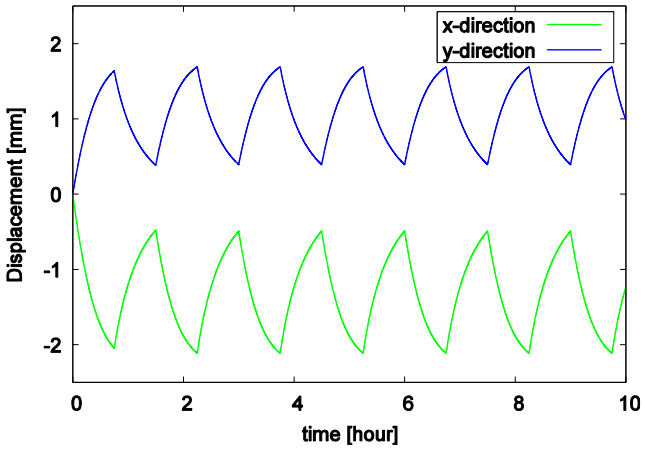

Fig. 13. Induced displacements by thermal disturbance given as step function

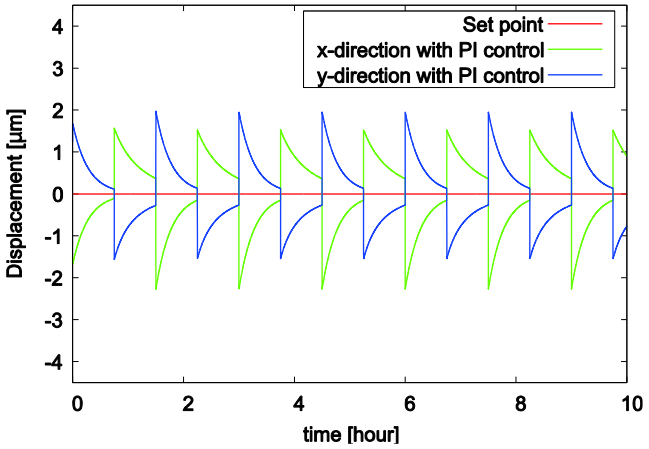

Fig. 14. Displacements controlled by PI controller in case 1

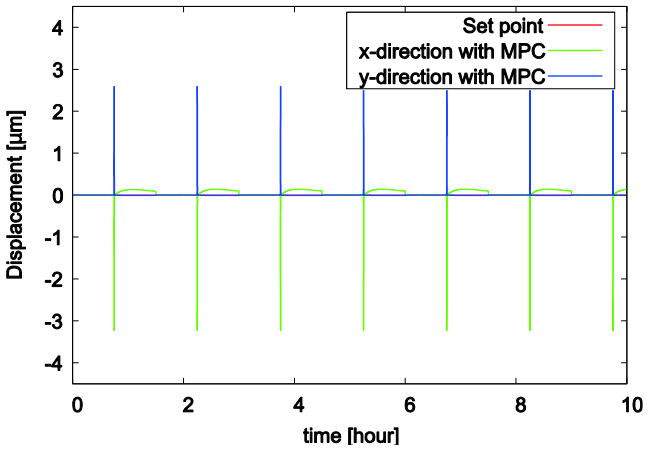

Fig. 15. Displacements controlled by MPC in case 1

Case 12: Thermal disturbance given as sinusoidal function

In case 2, we discuss the control behaviors when thermal disturbances are given as sinusoidal functions, as shown in Fig. 16. Figure 17 shows the induced displacements without a controller. In this case, the time history of the induced displacements has the shape of a sinusoidal function. The change rates of displacement are smoother than those in case 1.

Figure 18 shows the displacements controlled by the PI controller. Although large leaps such as those seen in case 1 are not generated, sinusoidal errors are generated periodically. For further improvement, differential feedback is also needed. Figure 19 shows the displacements controlled by the MPC controller. In the case of MPC, we can see neither large leaps nor periodic errors. This is because the thermal disturbances given as sinusoidal functions change smoothly in contrast with those given as step functions. As a result, MPC can give proper control heat inputs at all times, and the errors are almost zero.

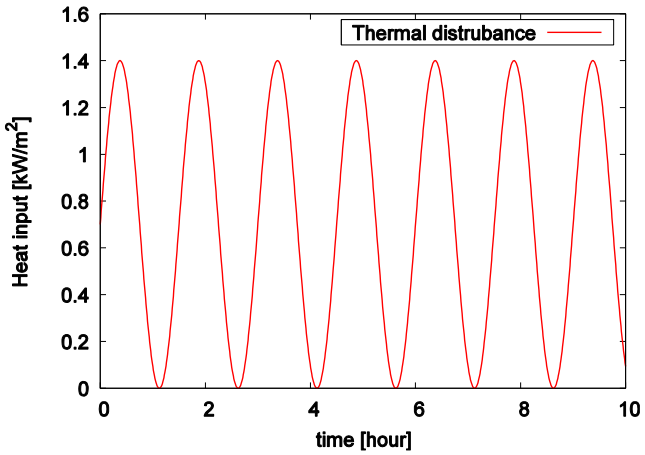

Fig. 16. Thermal disturbance given as sinusoidal function

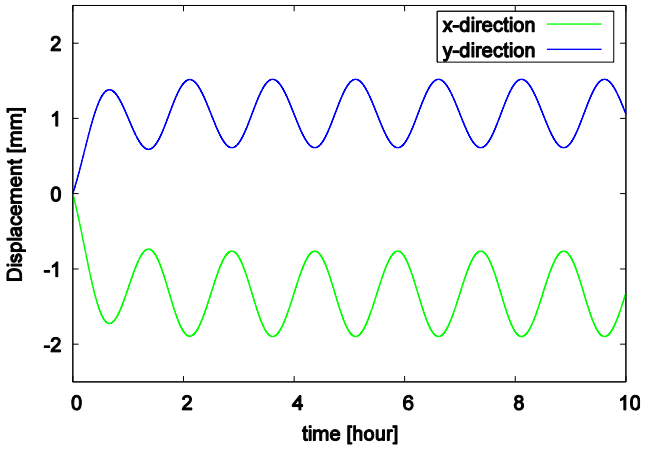

Fig. 17. Induced displacements by thermal disturbance given as sinusoidal function

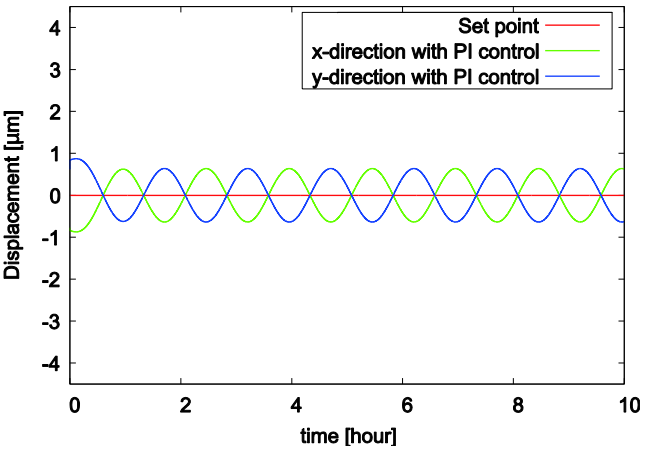

Fig. 18. Displacements controlled by PI controller in case 2

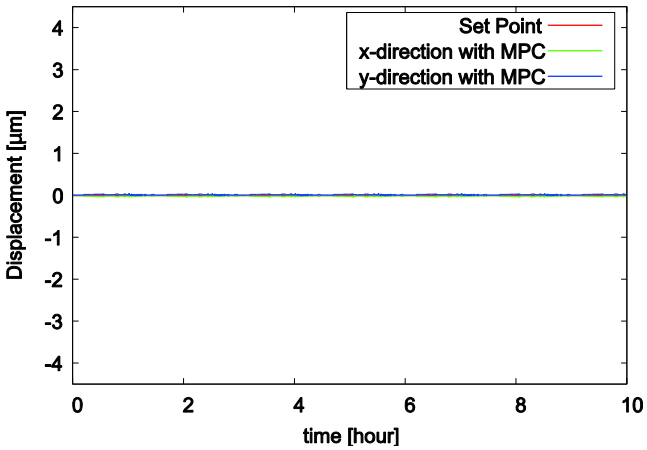

Fig. 19. Displacements controlled by MPC in case 2

5. Conclusion

We investigated a control system using artificial thermal expansion in order to maintain the pointing performance of a truss structure precisely. By focusing on the periodicity of the thermal deformation on orbit and the constraints of the control heat inputs, we adopted "Model Predictive Control" as feedforward control. In order to demonstrate its effectiveness, we analyzed the sensitivity of the control performance to various parameters using a rod model as an example of a simple structure. By comparing PI control and MPC, we showed that MPC has very high control performance against all of the parameters except for the case with a long period of thermal disturbance. However, it was also found that the controlled values have a small bias error in some cases because of modeling errors. In addition, other structural or actuation errors might occur in the control of a real structure. The control performance including these effects should be evaluated in future work. Finally, we attempted to control the truss structure in order to maintain pointing performance using both the PI and MPC controller. Through numerical simulations, it was found that MPC can control more precisely than PI control.

Declaration of conflicting interests

The authors declared no potential conflicts of interest with respect to the research, authorship, and/or publication of this article.

Funding

A part of this study was supported by "Study on Development of High-Precision Large Space Structural System" in the "Science and Engineering Experiments of Strategic Development and Research" of Institute of Space and Astronautical Science, Japan Aerospace Exploration Agency.

References

Agnes GS and Dooley J (2004) Precision deployable structures technology for NASA large aperture missions. In: Space 2004 conference and exhibit, San Diego, CA, 28 September – 9 October, pp. 5899-1–5899-7. Reston, VA: American Institute of Aeronautics and Astronautics.

Edberg DL (1987) Control of flexible structures by applied thermal gradients. AIAA Journal 25(6): 877–883.

Franklin GF, Powell DJ and Emami-Naeini A (2009) Feedback Control of Dynamic Systems. Upper Saddle River, NJ: Prentice Hall.

Givoli D and Rand O (1995) Minimization of thermoelastic deformation in space structures undergoing periodic motion. Journal of Spacecraft and Rockets 32(4): 662–669.

Haftka RT and Adelman HM (1985) An analytical investigation of shape control of large space structures by applied temperatures. AIAA Journal 23(3): 450–457.

Ishimura K, Akita T, Senba A, et al. (2011) Pointing control of truss structure by artificial thermal expansion. In: 19th space engineering conference, Kumamoto, Japan, 27–28 January, pp. J4-1–J4-4. Tokyo, Japan: The Japan Society of Mechanical Engineers. (in Japanese).

Ishimura K, Senba A, Iwasa T, et al. (2010) Prediction, measurement and stabilization of structural deformation on orbit. In: 61st international astronautical congress, Prague, 27 September–1 October, pp. 6116–6121. Red Hook, NY: Curran Associates.

Korkmaz S (2011) A review of active structural control: challenges for engineering informatics. Computers & Structures 8(23–24): 2113–2132.

Lake MS, Peterson LD, Hachkowski MR, et al. (1998) Research on the problem of high-precision deployment for large-aperture space-based science instruments. In: Space technology and applications international forum, Albuquerque, NM, 25–29 January, pp. 188–198. Melville, NY: AIP Publishing.

Maciejowski JM (2002) Predictive Control with Constraints. Upper Saddle River, NJ: Prentice Hall.

Miura K (1992) Adaptive Structures Research at ISAS, 1984–1990. Journal of Intelligent Material Systems and Structures 3(1): 54–74.

Pichler U and Irschik H (2001) Dynamic shape control of solids and structures by thermal expansion strains. Journal of Thermal Stresses 24(6): 565–576.

Puig L, Barton A and Rando N (2010) A review on large deployable structures for astrophysics missions. Acta Astronautica 67(1–2): 12–26.

Takahashi T, Mitsuda K, Kelley R, et al. (2010) The ASTROH mission. In: Space telescopes and instrumentation2010, San Diego, CA, 28 June–2 July, pp. 77320Z-1–77320Z-18. Bellingham, WA: SPIE.

Tolson RH and Huang JK (1992) Integrated control of thermally distorted large space antennas. Journal of Guidance, Control, and Dynamics 15(3): 605–614.

Utku S and Wada BK (1993) Adaptive structures in Japan. Journal of Intelligent Material Systems and Structures 4(4): 437–451.

Wada BK, Fanson JL and Crawley EF (1990) Adaptive structures. Journal of Intelligent Material Systems and Structures 1(2): 157–174